Article:
Zhao, S, Li, K, Yang, Z et al. (2022) A new power system active rescheduling method considering the dispatchable plug-in electric vehicles and intermittent renewable energies. Applied Energy, 314. 118715. ISSN: 0306-2619

https://doi.org/10.1016/j.apenergy.2022.118715

A New Power System Active Rescheduling Method Considering the Dispatchable Plug-in Electric Vehicles and Intermittent Renewable Energies

Shihao Zhao[a,b], Kang Li[c], Zhile Yang*[a], Xinzhi Xu[d], Ning Zhang[e]

[a]*Shenzhen Institute of Advanced Technology, Chinese Academy of Sciences, Shenzhen, Guangdong, 518055, China (e-mail: zyang07@qub.ac.uk,yj.guo@siat.ac.cn)*
[b]*Zhengzhou University, Zhengzhou, Henan, 450001, China (e-mail:shihao_zhao@126.com)*
[c]*School of Electronic and Electrical Engineering, University of Leeds, Leeds, LS2 9JT, UK (e-mail:k.li1@leeds.ac.uk)*
[d]*Global Energy Interconnection Development and Cooperation Organization, Beijing, 100034, China (e-mail:xinzhi-xu@sgcc.com.cn)*
[e]*Department of Electrical Engineering, State Key Lab of Power Systems, Tsinghua University, Beijing, China(e-mail:ningzhang@tsinghua.edu.cn)*

Abstract

The significant penetration of renewable power generations (RGs) and the large-scale use of plug-in electric vehicles (PEVs) have brought tangible impacts in tackling the climate change challenge the mankind has been facing due to substantive green-house gas and pollutant emissions from fossil-fuel based thermal power generation plants. However, the uncertainty of RGs has also exerted significant challenges to the grid operation and control. Therefore, dynamic power system scheduling to accommodate the intermittent RGs and mass roll-out of PEVs has become extremely important. In this paper, a novel power system rescheduling strategy is proposed to tackle this problem. Considering the uncertainty of the wind energy, a set of indices according to different wind power application scenarios is proposed to initiate a rescheduling scheme for power generations. In addition, a social learning particle swarm optimization algorithm based on real-value and binary parallel is proposed to schedule the output of generator units and the charging and discharging of the PEV. The effectiveness of the proposed active rescheduling framework and solving algorithm has been verified by extensive experiments considering different number of generating units and scenarios, achieving up to over 5.3% cost reduction. The experimental results have also shown that through expropriate management of the charging and discharging of PEVs would be significantly alleviate the negative impact on the grid stability caused by the intermittent wind power generations.

Nomenclature

a_j,b_j,c_j Coefficients of fuel cost for unit j

$CUT_{j,t-1}$ Continuous shutdown state time of unit j at time $t-1$

$CUT_{j,t-1}$ Continuous startup state time of unit j at time $t-1$

$F_{j,t}$ Fuel cost of unit j at time t

HPI High proportion index

LPI Low proportion index

MDT_j Minimum down time of unit j

MPI Medium proportion index

MUT_j Minimum up time of unit j

p_i^L Learning probability set by the algorithm

$P_{D,t}$ Power demand at time t

$P_{j,max}$ Maximum power limits of unit j

$P_{j,min}$ Minimum power limits of unit j

$P_{j,t}$ Determined power of unit j at time t

$P_{PEV,total}$ Total necessary charging power of PEVs

$P_{PEV,t}$ Demand of PEVs at time t

$P_{PEVC,t,max}$ Maximum charging power of PEVs at time t

$P_{PEVD,t,max}$ Maximum discharging power of PEVs at time t

SR_t Spinning reserves at time t

$SU_{C,j}$ Cold-start cost of unit j at time t

$SU_{H,j}$ Hot-start cost of unit j at time t

$SU_{j,t}$ Start-up cost of unit j at time t

$T_{cold,j}$ Cold-start hour of unit j

$TOFF_{j,t}$ Off-line duration time of unit j

$TON_{j,t}$ On-line duration time of unit j

TPC_{Tn} Total economic cost

$u_{j,t}$ Binary status of unit j at time t

$x_{i,j}(t)$ j^{th} dimension of the i^{th} individual in the t^{th} iteration

PEV Plug-in electric vehicles

RGs Renewable generations

UC Unit commitment

1. Introduction

Many countries worldwide are still heavily reliant on the fossil fuels such as coal and oil as the primary energy sources to power their economy due to the low cost, high flexibility and wide distribution of these energy resources, and some countries also rely mainly on thermal power plants for heating and supplying electricity [1]. Fossil fuel consumptions generate significant greenhouse gas (GHG) emissions [2]. Specifically, electricity generation and transportation are the two main sectors of GHG emissions [3]. Promoting clean energy and popularizing the use of PEVs have become important measures to reduce the GHG emissions. The development of RGs has huge potentials and is expected to meet two-thirds of the world's energy demand in the future, adding that the large-scale use of PEVs also greatly reduce the GHG emissions caused by the internal combustion engine based vehicles. The both sectors therefore become priority choices in the future decarbonization journey. However, the rapid development of PEV and RGs also bring new challenges to the power system operation and control. On the one hand, when random renewable energy sources such as wind energy are integrated into the power system on a large scale, they may bring great challenges to the dispatching of the power system [4]. On the other hand, the random charging behavior of large-scale PEV also have a direct impact on the supply and demand balancing of the power grid. Therefore, it is indispensable to develop new tools to seamless accommodate the RGS and PEVs.

As one of the most important tasks in power system, the unit commitment (UC) aims to schedule fossil fuel based power plants. It is considered as an NP hard problem due to its complexity, binary switching effect and constraint [5, 6]. When solving low-dimensional and less-constrained UC problems, traditional mathematical methods have been widely adopted such as dynamic programming methods [7], mixed integer programming methods [8, 9], integer programming methods [10], branch and bound methods [11], and Lagrange relaxation methods [12, 13]. These methods are easy to implement and have been incorporated in related solvers for solving low-dimensional UC problems. However, these methods are often difficult to solve high-dimensional and multi-constrained UC problems. Compared with the traditional mathematical methods, meta-heuristic algorithms (MAs) are compatible to achieve better results in solving optimization problems because of its flexible coding method and preferential optimization process. Moreover, the superiority of MA in search efficiency and flexibility of problem modeling have been widely verified [14]. Conventional MA algorithms include simulated annealing algorithm (SA) [15], genetic algorithm (GA) [16], differential evolution algorithm (DE) [17, 18], ant colony optimization algorithm (ACO) [19], particle swarm algorithm (PSO) [20], social learning particle swarm algorithm (SLPSO) [21], firefly algorithm [22], reinforcement learning [23] and so on. In addition, due to that the switch state of the unit is a binary variable, improved optimization algorithms based on binary coding or mixed binary and real number coding schemes have also used to solve the UC problem, such as binary differential evolution (DBDE) [24], binary competitive group optimization algorithm (BCSO) [25], binary gravitational search algorithm (BGSA) [26], binary grey wolf optimiser (BGWO) [27], mixed binary-continuous particle swarm optimization [28] and etc. Though MA methods are shown to have better capability than traditional mathematical methods in solving UC problems, large-scale and multi-dimensional optimization problems may cause MAs falling into the local optimum. In light of this, it is necessary to develop and improve the MA methods to solve the UC problems when the complexity the power system is rapidly increasing.

Wind energy is one of the most important renewable energy sources and a major substitute for traditional energy sources such as coal and petrol. However, due to the high degree of unpredictability and variability of the wind power, once largely integrated into the grid, wind power may cause significant challenges to system operators [29] from safety, reliability and operating efficiency perspectives [30], which further deteriorate the complex power system scheduling problem. Quan et al. [31] proposed a comprehensive computing framework for integration and quantification of distributed power systems to reduce the negative impact of wind energy and other intermittent renewable energy on the power system. Lin et al. [32] constructed a data-adaptive robust unit commitment model under high wind power penetration to obtain the economic unit scheduling plans. Diuana et al. [33] analyzed the influence of wind power penetration on the operating costs, electricity prices and GHG emissions of the power system in southern Brazil, and established relevant economic dispatch models. Mohasha et al. [34] built a stochastic robust UC model and analyzed the influence of uncertainty RGs on UC problems. Jin et al. [35] proposed an economic emission dispatch model that considered the carbon prices and uncertainty of wind power, and quantified the potential scale of wind energy with carbon prices to explore a balanced power dispatch strategy with the integration of the wind power. However, the weather-dependent nature of wind power makes wind forecasting a highly demanding and complex process [36]. Cobos et al. [37] proposed a multistage robust UC method with non-fixed resources, which was used to solve the wind energy uncertainty problem in the power generation plans. How to effectively eliminate the negative impact of wind energy on power system dispatch is still a problem that needs to be solved urgently.

With the rapid increase of the scale of RGs and PEV, it is also necessary to consider the impact of their access to the power system when solving the UC problems. The uncertainty of RGs [38, 39, 40] and the random charging behavior of PEV [41, 42, 43] also may bring challenges to the safety, stability and economy of the power system. Therefore, the traditional day-ahead scheduling method of power system has been difficult to meet the demand. On this basis, to reschedule the system under featured circumstances become a crucial solution. The concept of rescheduling comes from the scheduling theory and rescheduling methods have been widely adopted in many engineering fields such as manufacturing [44, 45, 46, 47] and transportation industry [48, 49, 50]. Carlos et al. [44] proposed a rescheduling mechanism that satisfied distributed constraints and contract network protocols to improve the adaptability of production systems to unpredictable order requirements. Zhang et al. [45] applied a rescheduling decision model based on fuzzy neural network of semiconductor manufacturing system (SMS) to adapt to its high dynamics and unpredictability. Xu et al. [46] proposed a rescheduling mechanism for mid-term maintenance of equipment to enable the equipments to pro-actively perform maintenance tasks in advance to prevent failures. Luo et al. [47] proposed a rescheduling scheme which allowed rejection to adapt to the possible problem of delayed arrival of work tasks. In order to improve the operation efficiency of railway transportation, Estelle et al. [48] proposed a train rescheduling method for dense railway systems. Li et al. [49] designed an integrated rescheduling model of production and delivery to deal with the unexpected situation that may occur in the process of cargo transportation. Kuppusamy et al. [50] designed a new train timetable rescheduling model to reduce the impact of accidents on subway operation efficiency. Taking into account the randomness of truck arrival time, Mohammad et al. [51] set up a rescheduling optimization mechanism for the terminal, which effectively improved the efficiency of unloading and loading at the terminal. Zhan et al. [52] propose a high-speed railway rescheduling framework based on dynamic programming algorithm, which improves the efficiency of high-speed railway operation management. Wang et al. [53] considered the security constraints of the power grid and proposed a rescheduling framework based on migration reinforcement learning to optimize the real-time active and reactive power of the power grid. In this paper, the rescheduling mechanism for wind energy uncertainty is applied to power system scheduling.

Inspired by the aforementioned rescheduling strategies, this paper introduces a novel active rescheduling strategy for power system scheduling, where the integrations of RGs and PEV are considered, so as to reduce the adverse effects of these uncertain factors. Unlike the rolling horizon scheduling of power systems, in the strategy design, different thresholds are designed according to the scale of installed wind power capacity to launch the rescheduling. The power system will be rescheduled only if the difference between the actual wind energy and the predicted wind energy used for day-ahead scheduling is larger than the set threshold. The scheduling problem is formulated as the UC problem where a binary and real value parallel

optimization framework to schedule the output of units and the charging and discharging management of PEVs simultaneously, and a highly efficient MA e.g. social learning particle swarm optimization is adopted. The negative influence of wind power and PEVs on the power system are therefore minimized through the combination of the day-ahead scheduling and intra-day scheduling, at the same time, it also avoids the influence of frequent rescheduling on the security and stable operation of the power system. The main contributions of this paper are as follows:

- A novel active rescheduling model is formulated for the first time for power systems, taking into account of the uncertainties of real-time wind power and intelligent charging and discharging of PEVs.
- Indices for assessing different application scenarios of wind energy uncertainty are designed, based on which the power system are rescheduled.
- The effectiveness of the proposed rescheduling framework assisted with the social learning particle swarm optimization method was verified by extensive experiments considering different uncertainty scenarios. The influence of wind energy and PEV on the power grid is analyzed in detail, and the effect of charging and discharging of PEVs on mitigating the negative influence of wind energy on the power system is thoroughly evaluated.

The remainder of this paper is organized as follows. Section 2 introduces the UC problem formulation considering wind energy and PEVs, and the active rescheduling method is presented in detail; Section 3 details the proposal of the social learning particle swarm optimization framework. Section 4 presents the experimental results and corresponding analysis. Section 5 concludes the paper.

Table 1: Unit commitment benchmark data settings

	Unit1	Unit2	Unit3	Unit4	Unit5	Unit6	Unit7	Unit8	Unit9	Unit10
Pmax(MW)	455	455	130	130	162	80	85	55	55	55
Pmin(MW)	150	150	20	20	25	20	25	10	10	10
a($ /h)	1000	970	700	680	450	370	480	660	665	670
b($ /MWh)	16.19	17.26	16.6	16.5	19.7	22.26	27.74	25.92	27.27	27.79
c($ /MWh^2)	0.00048	0.00031	0.002	0.00211	0.00398	0.00712	0.00079	0.00413	0.00222	0.00173
MUT(h)	8	8	5	5	6	3	3	1	1	1
MDT(h)	8	8	5	5	6	3	3	1	1	1
SU_H($)	4500	5000	550	560	900	170	260	30	30	30
SU_C($)	9000	10000	1100	1120	1800	340	520	60	60	60
$T_{cold}(h)$	5	5	4	4	4	2	2	0	0	0
Initial Status(h)	1	1	0	0	0	0	0	0	0	0

2. Problem formulation

The generator units considered in this paper are traditional thermal generator units. The fossil fuel cost of the units operating for one day is usually defined as the objective function of the UC problems. Due to the physical constraints of the unit itself and the safety requirements, the unit must meet necessary constraints. These constraints usually include power demand constraints, spinning reserve constraints and upper and lower limits of generating capacity of each unit etc. In addition, since PEVs and wind energy are also considered in this paper, their own constraints and their impacts on the conventional power system constraints should also be considered. This section mainly introduces the objective function and major constraints.

2.1. Objective function

The fossil fuel cost consumed by the thermal generating unit for 24 hours is taken as the objective function, and the interaction between the hourly costs is not considered. Without considering power loss, the objective function of UC problem can be defined as:

$$Cost = min \sum_{t=1}^{T} \sum_{j=1}^{n} [F_j(P_{j,t}) s_{j,t} + SU_{j,t}(1 - s_{j,t-1}) s_{j,t}] \tag{1}$$

In (1), *cost* represents the total generation cost of the unit, which can be divided into the fossil fuel cost consumed during the operation of the unit and the start-up cost of the unit. $P_{j,t}$ is the amount of electricity generated by the j^{th} unit at hour t. $F_j(P_{j,t})$ is a function of the cost of the fossil fuels consumed while the units are operating. The fuel cost function can be expressed as follows:

$$F_{j,t}(P_{j,t}) = a_j + b_j P_{j,t} + c_j P_{j,t}^2 \tag{2}$$

where a_j, b_j and c_j are the fuel cost coefficients of the j^{th} unit.

The start-up cost of the unit is expressed by $SU_{j,t}(1-u_{j,t-1})s_{j,t}$ in the objective function. $s_{j,t}$ represents the current state of the unit, and the on-off state is represented by 1 and 0 respectively. If the unit was in the shutdown state at the previous time interval and the current state is in the power-on state, then the start-up cost needs to be counted. In other cases, the start-up cost is 0. According to the time that the unit is in shutdown state before restarting, the start-up cost of the unit can be divided into hot start-up cost and cold start-up cost, which can be shown as follows:

$$SU_{j,t} = \begin{cases} SU_{H,j}, \ if \ MDT_j \leq CDT_{j,t} \leq MDT_j + T_{cold,j} \\ SU_{C,j}, \ if \ CDT_{j,t} > MDT_j + T_{cold,j} \end{cases} \tag{3}$$

Due to the physical conditions of the unit itself, the unit can not be started immediately after shutdown. MDT_j represents the minimum downtime of the unit, $T_{cold,j}$ represents the threshold of cold start time, and $CDT_{j,t}$ is the continuous shutdown time of the unit. If the shutdown time of the unit is greater than the minimum downtime and less than the sum of the minimum downtime and the cold start threshold time, the unit is defined as the hot start mode, which can be represented by $SU_{H,j}$. If the shutdown time of the unit is greater than the sum of the minimum shutdown time and the cold start threshold time, it is defined as the cold start mode, which is denoted by $SU_{C,j}$.

2.2. Constraints

This paper mainly introduces several constraints of the UC problem considering the influence of wind energy and PEVs, as well as their own constraints.

2.2.1. Power balance constraints

Considering the wind power and PEVs are integrated into the power grid, the generation of conventional units plus wind power should be equal to the traditional load plus the load required by PEVs. It is worth noting that in order to reduce the impact of the uncertainty of PEV charging on the power grid, the management of the charging and discharging of PEVs are taken into account. Therefore, two modes for PEVs are considered. One is grid-to-vehicle (G2V) where the load of PEVs is a positive real number. The other is vehicle-to-grid (V2G), which was introduced in [54], and the load of PEV is a negative real number. The formula for the power balance constraint is therefore given as follows:

$$\sum_{j=1}^{n} P_{j,t} s_{j,t} + P_{wind,t} = P_{D,t} + P_{PEV,t} \tag{4}$$

In (4), $\sum_{j=1}^{n} P_{j,t} s_{j,t}$ represents the power generation of all units at hour t, and $P_{wind,t}$ represents the wind energy connected to the grid at hour t. $P_{D,t}$ and $P_{PEV,t}$ represent the traditional load and the load demand of PEVs at hour t respectively.

2.2.2. Upper and lower limits of generating capacity

Generation units all have their physical limits, and these are often defined as the upper and lower limits of the generating capacity of the unit as shown below:

$$s_{j,t}P_{j,min} \leq P_{j,t} \leq s_{j,t}P_{j,max} \tag{5}$$

where $P_{j,min}$ and $P_{j,max}$ are the lower limit and upper limits of the production capacity of the j^{th} unit respectively.

Since the proposed model takes into account not only the conventional unit but also the wind energy, the upper and lower limits of wind energy also need to be considered, which can be shown in Formula (6):

$$0 \leq P_{wind,t} \leq P_{wind,max} \tag{6}$$

The wind power generation completely depends on the external environment and the size of installed capacity, so the upper limit of the wind power generation is the installed capacity of wind power generation, which is represented by $P_{wind,max}$. When the wind is too low, or even there is no wind, the wind energy can be ignored, denoted by 0.

2.2.3. Minimum up/down-time limits

The physical limitations of a generation unit itself determines that it is impossible for the unit to immediately change the state of starting up and shutting down, and there are minimum up/down-time limits for these units which can be defined below:

$$u_{j,t} = \begin{cases} 1, & if\ 1 \leq CUT_{j,t-1} < MUT_j \\ 0, & if\ 1 \leq CDT_{j,t-1} < MDT_j \\ 0\ or\ 1, & otherwise \end{cases} \tag{7}$$

where $CUT_{j,t-1}$ and $CDT_{j,t-1}$ respectively indicate the time when the unit is in continuous startup state and continuous shutdown state. MUT_j and MDT_j indicate the minimum time that the unit is on and off, respectively. As long as the unit is in the continuous start-up state for less than the set minimum up-time, the unit must remain in the start-up state, and vice versa.

2.2.4. Spinning reserve constraints

In order to meet the demand of unexpected load, the power plant usually needs to reserve a certain amount of power, which is important to ensure the safety and stable operation of the power system. This can be formulated below,

$$P_{D,t} + P_{PEV,t} + SR_t \leq \sum_{j=1}^{n} P_{j,max}s_{j,t} + P_{wind,t} \tag{8}$$

$$SR_t = m \times P_{D,t}. \tag{9}$$

that is, the generating capacity of the unit and wind power should be approximately equal to or slightly greater than the sum of all load requirements and the spinning reserves. Spinning reserve is represented by SR_t, and relationship is shown by Formula (9). Based on the suggestions from [55] and the spinning reserve is set as 0.1 times the traditional load in this paper.

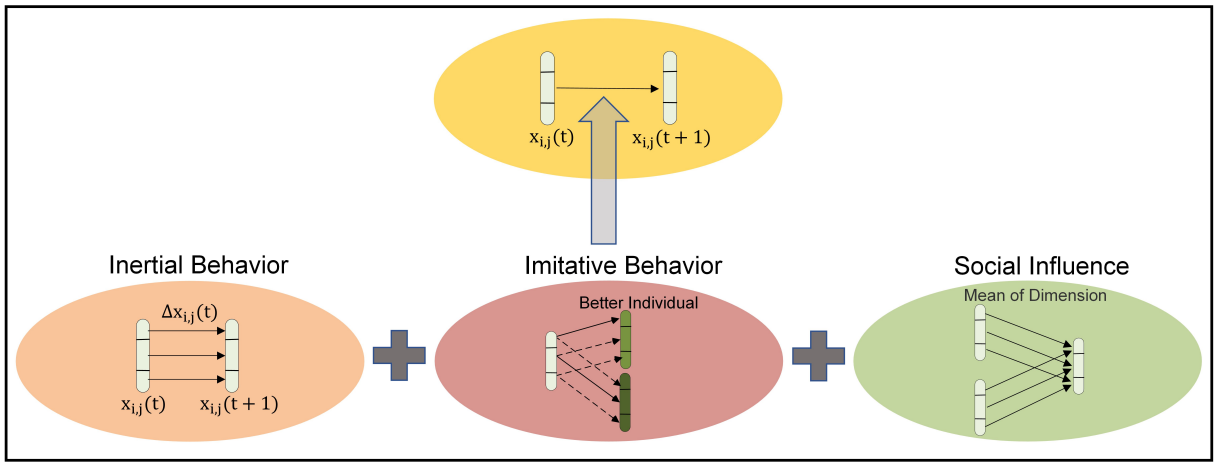

Figure 1: The learning mechanism of SLPSO.

2.2.5. Constrains of PEVs

Since PEVs are considered in this paper, their constraints need to be considered. Relevant constraints include charging and discharging capacity limits and power demand constraints of PEVs, which can be represented by formula (10) and (11) respectively,

$$P_{PEVD,t,max} \leq P_{PEV,t} \leq P_{PEVC,t,max} \tag{10}$$

$$\sum_{t=1}^{T} P_{PEV,t} = P_{PEV,total} \tag{11}$$

as shown in formula (10), $P_{PEVD,t,max}$ represents the maximum discharge capacity of all PEVs when discharging, and $P_{PEVC,t,max}$ represents the maximum charge capacity of all PEVs when charging. Formula (11) represents the total amount of electricity required to maintain the normal operation of PEVs in one day, and $P_{PEV,total}$ represents the total amount of charging demand of all PEVs in one day.

2.3. Active rescheduling indices considering wind energy uncertainty

The active rescheduling is defined as the scheme that the power system actively reschedule the unit commitment and corresponding plans given certain predefined circumstances during the intra-day scheduling time horizon. These circumstances are defined by indices related to the deviation scale of RGs such as wind energy from their expected generations.

The nature of wind energy dictates that it is difficult to be accurately predicted, and when the gap between actual wind power generation and predicted generation is sufficiently enough, if the power generations still follow the day-ahead dispatching schedule, it may imposes challenges to the power system operation and control, even affect the security and reliability.

To address above problems, this paper proposes to adopt a method combining day-ahead dispatching and intra-day rescheduling to address the negative impact of wind energy uncertainty. In this new scheme, when the large gap between the actual wind energy and the predicted value is sufficiently large, the power system will actively reschedule the output of generation units to adapt to the generation uncertainties introduced by wind energy and reduce the cost of power generation. This scheme is different from intra-day dynamic economic dispatch which schedule power outputs of generating units at fixed intervals within a day, e.g. every hour or even shorter interval. This is due to the fact that frequent rescheduling of the power system is computationally expensive and unnecessary, and in the worst scenario, it may even affect the reliability of

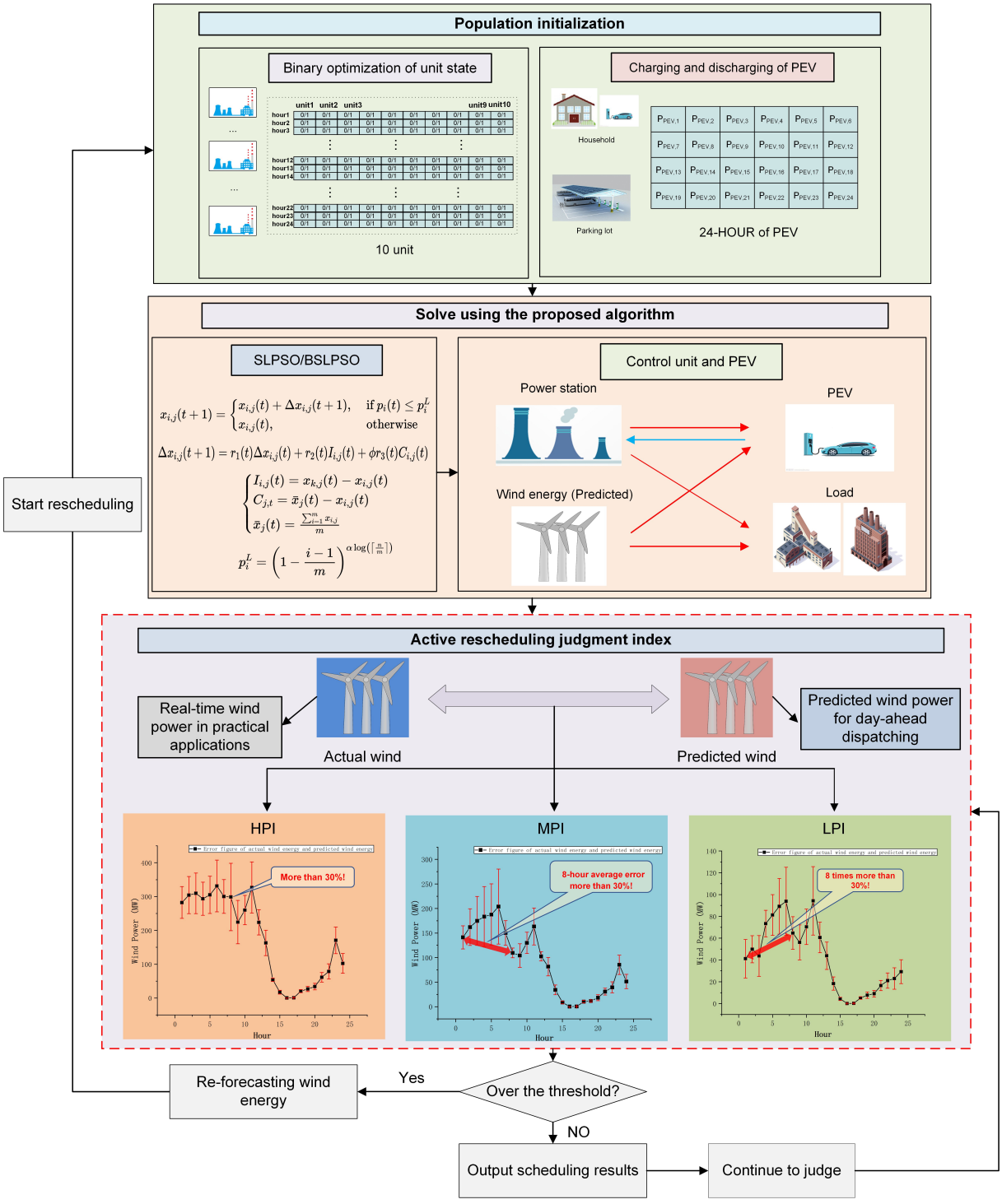

Figure 2: The proposed optimal framework.

the power system as frequent adjustment of the set-points of power systems may cause instability issues. To address this issue, this paper first defines several indices and thresholds for different application scenarios of wind energy. Only when the difference between the actual wind power generation and the predicted value exceeds certain thresholds, the rescheduling scheme is triggered otherwise the output of the unit still follow the previous dispatching schedule. This paper designs three indices elaborated below:

1) Fixed threshold for high proportion index (HPI) scenario: For areas where wind energy accounts for a relatively large proportion of the regional power generation, the power system will be rescheduled as long as the difference between the actual wind energy and predicted wind energy in a certain hour exceeds a given threshold. This paper stipulates that if the actual wind energy in a certain hour exceeds 30% of the predicted wind energy, the power system outputs will be rescheduled, which can be defined as follows:

$$RD_{HPI} = \begin{cases} 1, & if\ (wind_{a,t} - wind_{p,t})/wind_{p,t} \geq 30\% \\ 0, & otherwise \end{cases} \tag{12}$$

2) Average error for medium proportion index (MPI) scenario: For areas with large wind fluctuations, while wind power generation accounts for a relatively modest proportion of the overall generation capacity. Although a relatively modest amount of wind power may have not a substantial impact on power system dispatching even if the gap between actual wind power generation and predicted value is large, however frequent fluctuations of this gap still affects the power system operation and control. In this case, if the average error between the actual wind power and the predicted value exceeds a specified threshold, the power system generation profile will be rescheduled. In this scenario, this paper proposes that the average error between the actual wind energy and the predicted value should be calculated every 8 hours. If the average error exceeds 30% in 8 hours, rescheduling is considered necessary. This is formulated below:

$$RD_{MPI} = \begin{cases} 1, & if\ \frac{\sum_{t=1}^{8}(wind_{a,t} - wind_{p,t})/wind_{p,t}}{8} \geq 30\% \\ 0, & otherwise \end{cases} \tag{13}$$

3) Frequency for low proportion index (LPI) scenario: For areas where wind energy accounts for a relatively small proportion of the regional power generation profile. Due to the relatively small proportion of wind energy, even if the wind energy occasionally exceeds the given threshold, it does not have a significant impact on the entire power system operation. In this regard, there is no need to reschedule the power system dispatch. Therefore, only when the difference between the actual wind power and the predicted one exceeds a specified number of times of a given threshold, the active rescheduling is triggered. In this scenario, the index is initially set to 0. If the actual wind power in an hour exceeds 30% of the predicted wind power, the index is increased by 1. Then if the index reaches 8, the power system will be rescheduled, which can be formulated below:

$$RD_{LPI} = \begin{cases} 1, if\ times((wind_{a,t} - wind_{p,t})/wind_{p,t} \geq 30\%) \geq 8 \\ 0, \quad otherwise \end{cases} \tag{14}$$

RD_{HPI}, RD_{MPI} and RD_{LPI} represent the decision of rescheduling under the scenarios of high, medium and low wind energy proportions respectively. Specific threshold values and related calculation methods are shown in Table 2, where $wind_{a,t}$ represents the actual wind energy at t^{th} hour, and $wind_{p,t}$ represents the predicted wind energy at t^{th} hour. In this paper, if the installed capacity of wind energy accounts for more than 20% of the total power generation capacity of traditional units, it is defined as high proportion, 10% to 20% is defined as medium proportion, and less than 10% is defined as low proportion.

The parameters of the generation units used in this study was set according to [56], which are listed in Table 1.

3. Methodology

This section details the optimization framework proposed in this paper. Subsection 3.1 proposes the parallel SLPSO framework. Subsection 2.3 further elaborates on the rescheduling indices proposed for wind energy uncertainty.

3.1. Parallel social learning particle swarm optimization framework

The traditional PSO algorithm aims to find the optimal solution by allowing the particles to continuously approach the best position of the individual itself and the best position of all individuals [20]. The PSO has the features of easy implementation and fewer parameters to be adjusted, it has been widely used in solving various optimization problems [57]. However, it has also been shown that the conventional PSO often falls into the local optimal solution when it encounters the high-dimensional and large-scale optimization problems, and cannot achieve the desired resuls.

Table 2: Indices considering wind energy uncertainty.

Index	**Application Scenario**	**Computation method**	**Threshold**
Fixed Value	Wind Energy $\geq 20\%$	$(wind_{a,t} - wind_{p,t})/wind_{p,t}$	30%
Average Error	$10\% \leq$ Wind Energy $\leq 20\%$	$\frac{\sum_{t=1}^{8}(wind_{a,t}-wind_{p,t})/wind_{p,t}}{8}$	30%
Frequency	Wind Energy $\leq 10\%$	$times((wind_{a,t} - wind_{p,t})/wind_{p,t} \geq 30\%)$	8

The SLPSO improves the learning mechanism of traditional PSO. In each iteration, the individuals in the population are sorted according to their fitness values calculated by the fitness function, and individuals are only allowed to randomly learn from other individuals that are better than themselves. Such learning mechanism not only increases the diversity of the population when solving large-scale optimization problems and improves the ability of the algorithm to find the optimal solution, but also accelerates the convergence speed of the algorithm. Experiments have showed that SLPSO has good performance when facing high dimensional and large-scale problems [58]. Since the intelligent scheduling of large-scale electric vehicles is considered in this paper, the algorithm framework is designed based on SLPSO. According to the proposed problem model, this paper proposed a binary and real-value parallel optimization algorithm framework based on SLPSO. Binary SLPSO (BSLPSO) is used to optimize the on-off state of the unit, and real-value SLPSO is used to manage the charging and discharging of PEVs. The rest of this section specifically elaborates the SLPSO and BSLPSO.

The location update formula in SLPSO is given below:

$$x_{i,j}(t+1) = \begin{cases} x_{i,j}(t) + \Delta x_{i,j}(t+1), & \text{if } p_i(t) \leq p_i^L \\ x_{i,j}(t), & \text{otherwise} \end{cases} \tag{15}$$

$$p_i^L = (1 - \frac{i-1}{m})^{\alpha log(\lceil \frac{n}{m} \rceil)} \tag{16}$$

$x_{i,j}(t)$ represents the j^{th} dimension of the i^{th} individual in the t^{th} iteration. $\Delta x_{i,j}(t+1)$ is the update degree of the individual calculated by the above-mentioned learning mechanism during this location update. $p_i(t)$ is a random number between 0 and 1, and p_i^L is a learning probability set by the algorithm. The calculation of learning probability is shown in Formula (16), where n is the problem dimension, and m is the size of the population. It is evident that the learning probability will increase with the increase of the problem dimensions and population size, which can improve the robustness of the algorithm for problems of different dimensions and scales. α is the only parameter which needs to be set in SLPSO algorithm, which was set as 0.5 in this paper.

The learning mechanism of SLPSO can be reflected by Formulas (17), (18) and (19):

$$\Delta x_{i,j}(t+1) = r_1(t)\Delta x_{i,j}(t) + r_2(t)I_{i,j}(t) + \phi r_3(t)C_{i,j}(t) \tag{17}$$

$$\begin{cases} I_{i,j}(t) = x_{k,j}(t) - x_{i,j}(t) \\ C_{j,t} = \overline{x}_j(t) - x_{i,j}(t) \\ \overline{x}_j(t) = \frac{\sum_{i=1}^{m} x_{i,j}}{m} \end{cases} \tag{18}$$

$$\phi = 0.01 \times \frac{n}{m} \tag{19}$$

$r_1(t)\Delta x_{i,j}(t)$ is defined as inertial behavior, so that the individual can continue to update the current position according to the update degree of the previous iteration. $r_2(t)I_{i,j}(t)$ is defined as an imitative behavior, which makes the individuals randomly learn from other better individuals. $\phi r_3(t)C_{i,j}(t)$ is defined as social influence behavior, which makes the individual approach the average value of all individuals in a particular dimension. $r_1(t)$, $r_2(t)$ and $r_3(t)$ are all random numbers between 0 and 1. ϕ is related to the population size and dimension, and its calculation method is shown in (19). As shown in (18), $x_{k,j}(t)$ represents the j^{th} dimension of the k^{th} individual randomly selected from the better individuals in this iteration. $\overline{x}_j(t)$ represents the average value of the j^{th} dimension of all the individuals in this iteration. Inertial behavior, imitation behavior and social influence together constitute the complete learning mechanism of SLPSO. The specific learning mechanism is illustrated in Figure 1. This mechanism can not only increase the ability of exploitation, as well as the ability of exploration of the algorithm.

3.2. Binary conversion of SLPSO

The proposed algorithm needs a binary conversion function to convert each parameter of the individual to 0 or 1 after each position update. Popular binary conversion formulas are shown in Table 3:

Table 3: Five commonly used binary conversion formulas.

Name	Binary Function
BSLPSO-I	$Pr_{i,j} = \lvert erf(\frac{\sqrt{\pi}}{2}v)\rvert$
BSLPSO-II	$Pr_{i,j} = \lvert tanh(v)\rvert$
BSLPSO-III	$Pr_{i,j} = \lvert\frac{v}{\sqrt{1+v^2}}\rvert$
BSLPSO-IV	$Pr_{i,j} = \lvert\frac{2}{\pi}arctan(\frac{\sqrt{\pi}}{2}v)\rvert$
BSLPSO-V	$Pr_{i,j} = 2 * \lvert\frac{1}{1+e^{-x_{i,j}}} - 0.5\rvert$

By applying these five binary conversion methods to SLPSO, five binary SLPSO methods (BSLPSOs) can be obtained. These five methods are applied to the UC problem considering the charging and discharging of PEVs, and the convergence trajectories are shown in Figure 3. It is evident based on Figure 3 that the fifth binary conversion function has a better performance and helps SLPSO to find a better solution, therefore in the following the fifth binary conversion function is chosen in the following experimental studies. The specific conversion mechanism are given below:

$$Pr_{i,j} = 2 * \lvert\frac{1}{1+e^{-x_{i,j}}} - 0.5\rvert \tag{20}$$

$$x_{i,j} = \begin{cases} 1, & \text{if } rand < Pr_{i,j} \\ 0, & \text{otherwise} \end{cases} \tag{21}$$

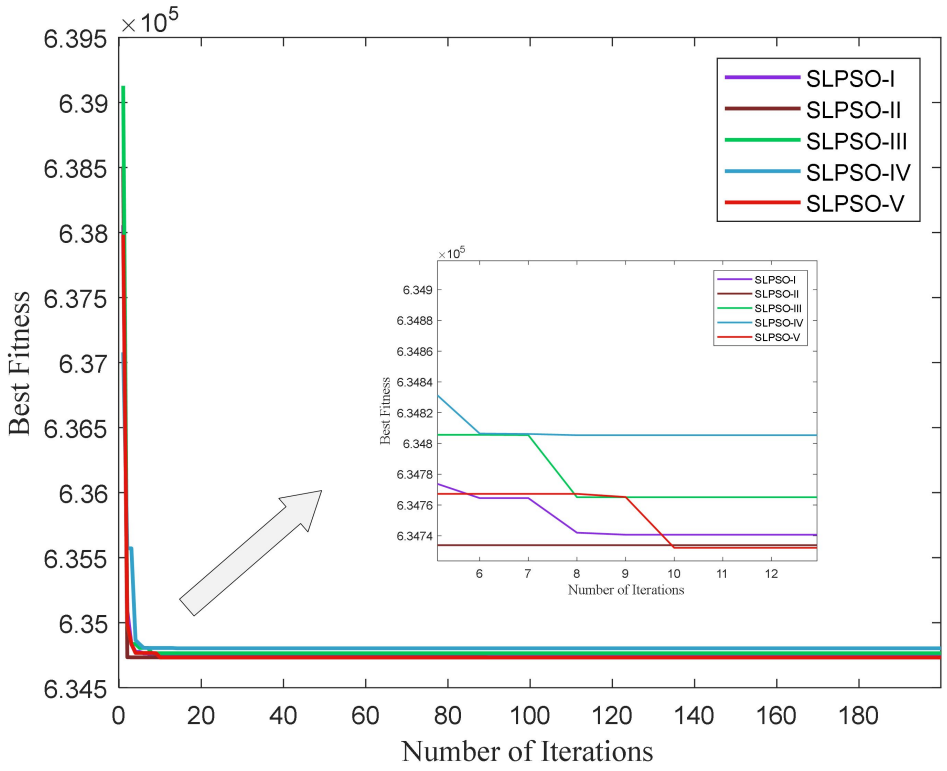

Figure 3: Convergence of the five SLPSOs applied to the UC problem considering the PEV scenario.

In (21), *rand* is a random number between 0 and 1, which is used to compare with the result calculated by the V-shaped function. This paper uses this mechanism to binarize SLPSO.

The framework proposed in this paper is summarized in Figure 2.

Table 4: Economic costs comparison between BSLPSO and BPSOs ($/day).

Units \ Methods	BSLPSO	BPSO	NBPSO	BLPSO	BCSO
10	**539209.44**	539569.18	539521.64	539602.56	539409.37
20	**1099295.45**	1108919.50	1111070.11	1107274.25	1099923.53
40	**2220799.62**	2252222.21	2271009.21	2273259.39	2220976.38
60	**3342015.99**	3399381.82	3449616.23	3439590.71	3342437.06
80	**4465156.98**	4548909.21	4629706.37	4633942.06	4465172.92
100	**5587136.37**	5699940.75	5810070.62	5813829.19	5587154.89

4. Experimental study and result analysis

In this section, three different cases are examined on *Matlab R2020a* to verify 1) the performance of the proposed algorithm; 2) the effectiveness of the proposed method in dealing with wind energy uncertainty scenarios; and 3) the management of PEV charging and discharging to fill the valley and reduce the peak of the load as well as to reduce the impact of wind energy uncertainty on the power grid.

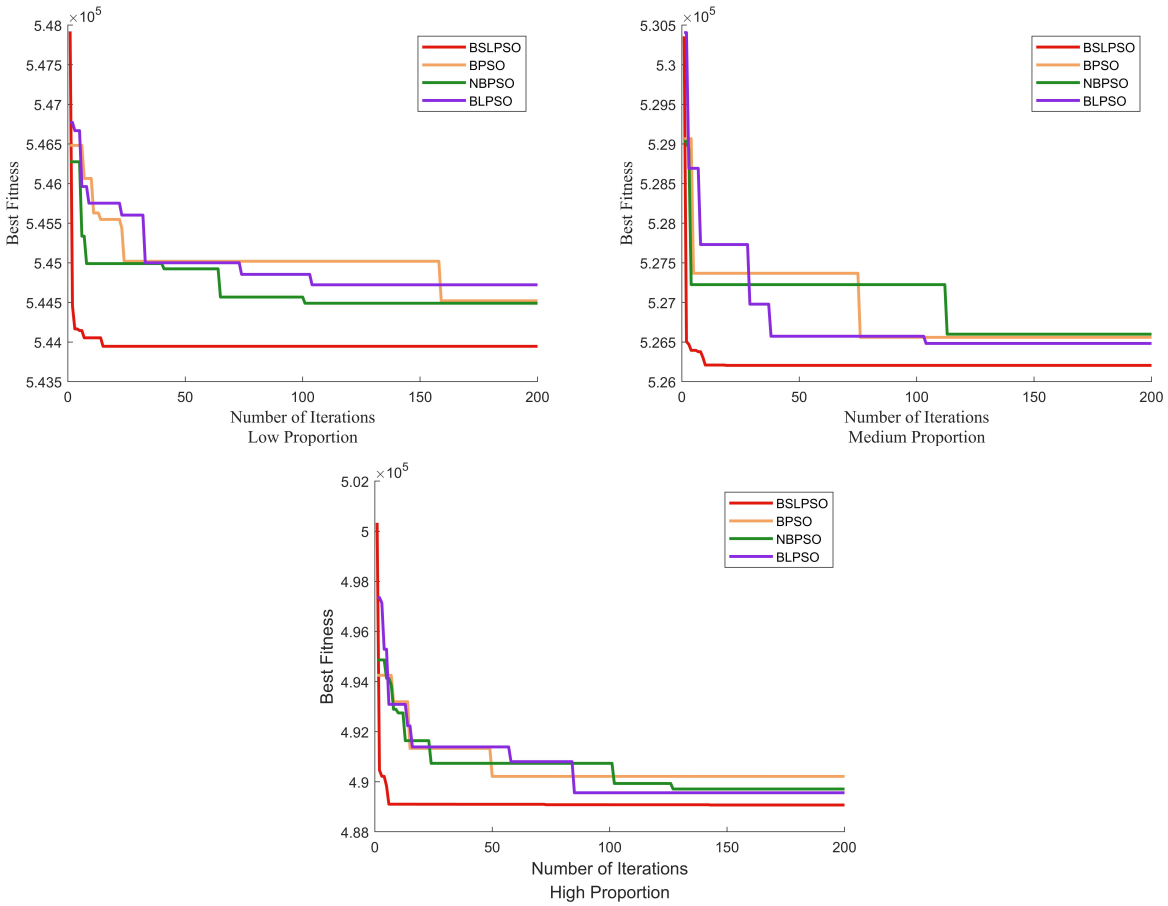

Figure 4: Comparison of BSLPSO and BPSOs on 10-unit benchmark with three wind energy application scenarios.

4.1. Case 1: The performance of BSLPSO in solving the UC problems considering wind energy integration

In this case, the forecast data of a typical spring day of a $85MW$ on-shore wind farm in Northern Ireland power system was selected [14], and the wind energy data was used in the UC problem. In order to verify the performance of the proposed optimization algorithm, the BSLPSO was applied to the aforementioned problem, and its performance was compared with the four PSO variants, including BPSO, BLPSO, NBPSO [59] and BCSO [25]. The comparison results are shown in Table 4. According to Table 4, BSLPSO always had a slight edge over BCSO. In addition, BSLPSO delivered a consistent performance and was always able to find the best results in solving problems with different numbers of generation units, and the advantages BSLPSO over the other three algorithms are getting more distinctive as the number of units increases. When there are only ten units, the minimum difference between the results of BSLPSO and the other algorithms is about 200 $\$/day$, but when the number of units reaches 100, the maximum difference has reached $226,291$ $\$/day$. It is worth mentioning that in the UC problem, the number of units determines the dimension of the UC problem. When there are only 10 units and only the economic cost of the units in 24 hours is considered, the dimension of the problem is $10 \times 24 = 240$, and when the number of units reaches 100, the dimension of the problem reaches to 2400. Table 4 has clearly demonstrated the performance of BSLPSO in solving UC problems, especially the high-dimensional UC problems.

To examine all the three wind energy application scenarios defined in the previous section, based on data from off-shore wind farms in Ireland, the hourly wind power data are first scaled up by the factor of 1.6, so that the peak value of wind power generation can account for about 10% of the total output of traditional units, and this allows the examination of the medium proportion of wind power scenario. These wind energy

generation profile of the medium proportion, can be further scaled up by a factor of 2 to obtain the high proportion scenario, or scaled down by a factor of 0.5 to obtain the low proportion scenario. These three wind power scenarios are incorporated in the 10-unit benchmark UC problem, and the optimization problem was then solved by the BSLPSO and the three aforementioned PSO variants. The resultant convergence trajectories of the 10-unit benchmark UC problem under the three wind power generation scenarios are illustrated in Figure 4. In Figure 4, the trajectory in red are the solutions of the BSLPSO, it is clear that the BSLPSO can find better results than the other three algorithms in all three scenarios, and all have the fastest convergence rate, which confirm the performance of BSLPSO in solving UC problems in different wind generation scenarios. In summary, the BSLPSO can not only solve the UC problem of different dimensions satisfactorily, but also well adapt to the UC problems in different wind power generation scenarios.

Table 5: Wind energy experimental data under three scenarios.

Application scenario	**Day-ahead predicted data**	**True wind power data**	**New predicted data**
Low proportions scenario	$0.8 \times wind_{spring}$	$rand \times wind_p$ $(0.7 \leq rand \leq 1.6)$	$1.3 \times wind_p$
Medium proportions scenario	$1.6 \times wind_{spring}$	$rand \times wind_p$ $(1.2 \leq rand \leq 1.6)$	$1.3 \times wind_p$
High proportions scenario	$3.2 \times wind_{spring}$	$rand \times wind_p$ $(1.1 \leq rand \leq 1.5)$	$1.3 \times wind_p$

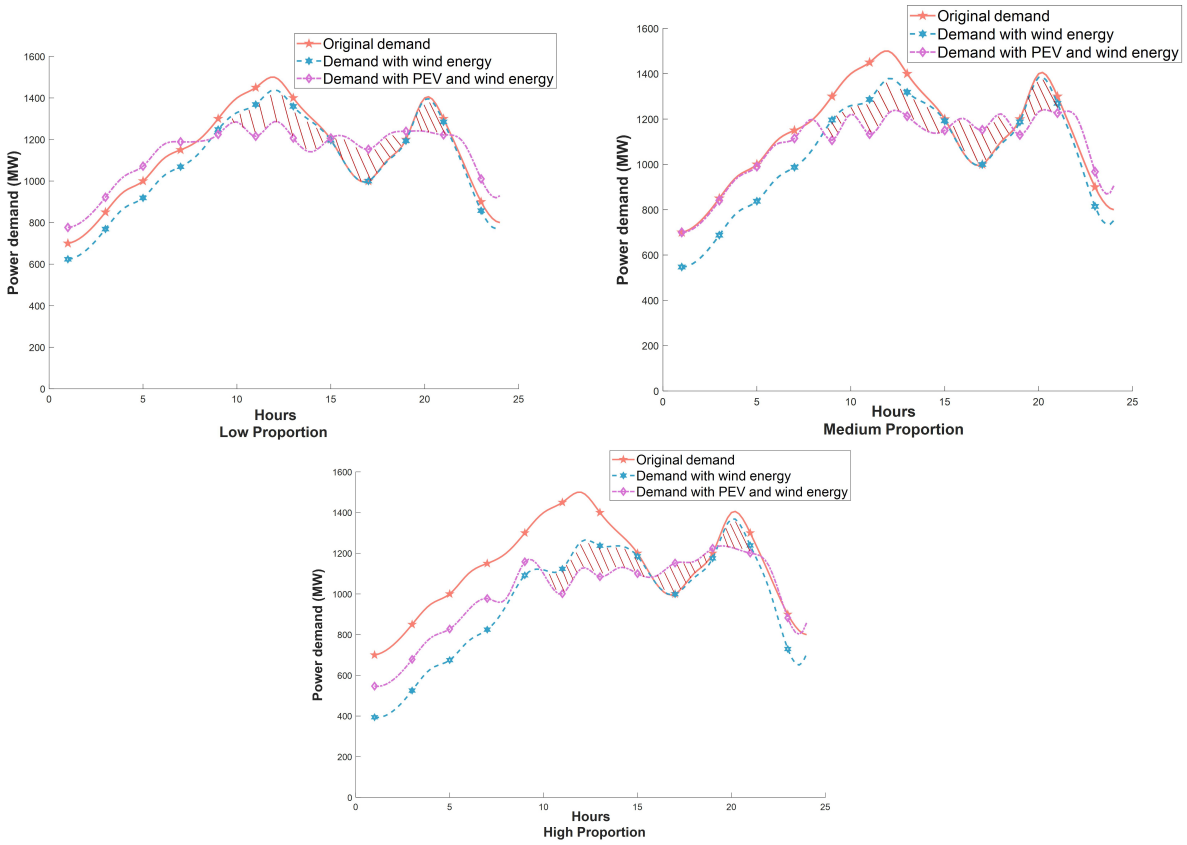

Figure 5: Simulation results of 10-unit benchmark UC problem with PEV in three wind energy application scenarios.

4.2. Case 2: Benefits of appropriate management of PEV charging and discharging on power system integrated with wind energy

Due to the uncertainty of wind energy, for a power system with higher proportion of wind power generation capacity, low load demand may bring severe challenges to the balancing of the power grid. Therefore, to intelligently manage the charging and discharging of PEV to fill the valley and to shave the peak of the grid load is vital to improve the stability of the power system and to mitigate the negative impact of wind energy uncertainty on the power grid.

According to [3], the average daily mileage of a PEV is about 32.88 miles, so a scenario is set with a total of 150,000 PEVs, and the average daily charge demand of PEV is $7.427kWh$, then the total daily power demand of all PEVs is about $1.114GWh$. This paper sets the battery capacity of PEVs as 30kWh, the state of charge (SOC) during charging or discharging as 50%, the number of PEV charging and discharging per hour as 20% of the total PEVs, and the charging efficiency as 85%. Thus, the maximum power for PEV charging and discharging per hour will be $153MW$ and $-153MW$ respectively.

Under the three wind power generation scenarios, the PEV charging and discharging results after rescheduling obtained by the proposed optimization algorithm are listed in Table 6. In Table 6, the data highlighted in purple indicate the discharge power, and data highlighted in green are discharging power. It is evident that PEVs are managed to charge during the load valley period while discharge during the load peak period. In addition, as shown in Table 6, during the load valley period from 1^{th} to 8^{th} hour, the wind may provide an excessive amount of electricity, which will bring challenges to the supply and demand balancing. By charging the PEV as a load during this time period, the energy provided by the wind can be consumed, thereby improving the stability of the power system. It is also evident from Figure 5 that wind energy cannot help with peak-shaving and valley-filling of the grid load, while the peak-shaving and valley-filling of the power grid can be achieved through intelligent charging and discharging of PEV is added PEVs. This confirms that intelligent charging and discharging of PEVs can play an important role in maintaining the balance between supply and demand of the power grid and alleviating the negative impact of wind energy uncertainty on the power system.

4.3. Case 3: Comprehensive UC problems with integration of wind energy and PEVs before and after rescheduling

This case study presents a comparative analysis of unit output, grid load and economic cost before and after rescheduling, and the benefits of rescheduling on the economy and reliability of the power system are investigated in detail. The comparison of different UC problems under the three scenarios are shown in Figure 6.

In the experiments only one new wind energy forecast is conducted, and the difference between the new predicted wind power generation data and the real wind generation data is below the threshold, which implies that the system only needs to be rescheduled once. The experimental data used in the three wind energy scenarios can be found in Table 5, where $wind_{spring}$ represents the wind power data of the typical spring day of on-shore power plants in Northern Ireland as mentioned in Case 1, $wind_p$ represents the day-ahead forecast data of the wind power. *rand* is a random number. The wind energy data of the three scenarios are shown in Figure 6a.

When there is a large gap between the actual wind energy and the predicted wind energy, it is necessary to arrange the rescheduling of the power system. If the actual wind energy is far less than the predicted wind energy, it is unacceptable to continue to use the day-ahead dispatching plan. However, if the actual wind energy is much greater than the predicted value, the electric energy provided by the power grid will be greater than the demand, which will bring challenges to the security and economy of the power system. This paper mainly considers the situation where the actual wind energy is greater than its predictions.

Figure 6b shows a comparison of the grid load before and after rescheduling, the grid load here is the traditional load plus PEV load and minus the wind power. It can be evident that the grid load after rescheduling is lower than before rescheduling in most periods, this is due to the integration of wind energy and intelligent management of charging and discharging of PEVs after rescheduling. This confirms again that rescheduling is helpful to reduce the load of the power grid. In addition, rescheduling also helps to reduce

Table 6: New forecast data of wind energy and PEV charging and discharging after rescheduling.

Hour	High Proportion Wind (MW)	Medium Proportion Wind (MW)	Low Proportion Wind (MW)	High Proportion PEV Load (MW)	Medium Proportion PEV Load (MW)	Low Proportion PEV Load (MW)	Traditional Load (MW)
1	305.93	152.96	76.48	153	153	153	700
2	324.19	162.09	81.04	153	153	153	750
3	324.60	162.30	81.15	153	153	153	850
4	317.99	158.99	79.50	153	153	153	950
5	325.19	162.59	81.30	153	153	153	1000
6	331.30	165.65	82.83	153	153	152.85	1100
7	325.35	162.68	81.34	153	127.51	120.09	1150
8	258.92	129.46	64.73	35.10	127.96	55.83	1200
9	208.42	104.21	52.10	66.65	-89.33	-23.24	1300
10	281.59	140.79	70.40	-19.26	-37.12	-45.39	1400
11	326.73	163.36	81.68	-122.12	-153	-153	1450
12	242.49	121.24	60.62	-132.15	-153	-153	1500
13	163.07	81.54	40.77	-152.33	-105.95	-152.59	1400
14	63.56	31.78	15.89	-107.75	-118.83	-143.28	1300
15	14.98	7.49	3.74	-85.26	-42.37	11.09	1200
16	0.46	0.23	0.11	38.79	153	152.86	1050
17	0.87	0.44	0.22	153	152.88	152.99	1000
18	20.51	10.25	5.13	79.41	133.24	126.04	1100
19	25.04	12.52	6.26	49.67	-57.48	45.82	1200
20	31.49	15.74	7.87	-139.63	-152.12	-152.68	1400
21	61.40	30.70	15.35	-37.78	-42.69	-62.39	1300
22	73.09	36.54	18.27	110.87	147.52	111.23	1100
23	170.60	85.30	42.65	153	153	153	900
24	95.14	47.57	23.78	153	153	153	800

the generation cost of the power system, as shown from the changes in the outputs of some conventional thermal generation units before and after rescheduling as illustrated in Figure 6c. The outputs of units are directly related to the load of the power grid. Therefore, when the actual wind energy is greater than its predictions made in the previous day, the output of some units after rescheduling will be less than the output of units during the day-ahead dispatching, which is clearly reflected in the output changes of several thermal units as shown in Figure 6c. Table 7 shows the comparison of the economic costs consumed by the unit operating for one day before and after rescheduling in the three scenarios. It is shown in the table that the economic cost after rescheduling is often lower than before rescheduling, and the economic improvement

Table 7: Comparison of the economic costs of a day before and after rescheduling in different scenarios ($/day).

Wind energy application scenario	Cost of day-ahead scheduling	Cost of rescheduling	Difference
Low proportions scenario	594208.31	585564.15	1.4%
Medium proportions scenario	566856.68	553229.87	2.4%
High proportions scenario	532534.56	504184.86	5.3%

after rescheduling will increase as the proportion of wind energy increases. Therefore, rescheduling of the power system is helpful to relieve the load pressure of the power grid and reduce the cost of power generation.

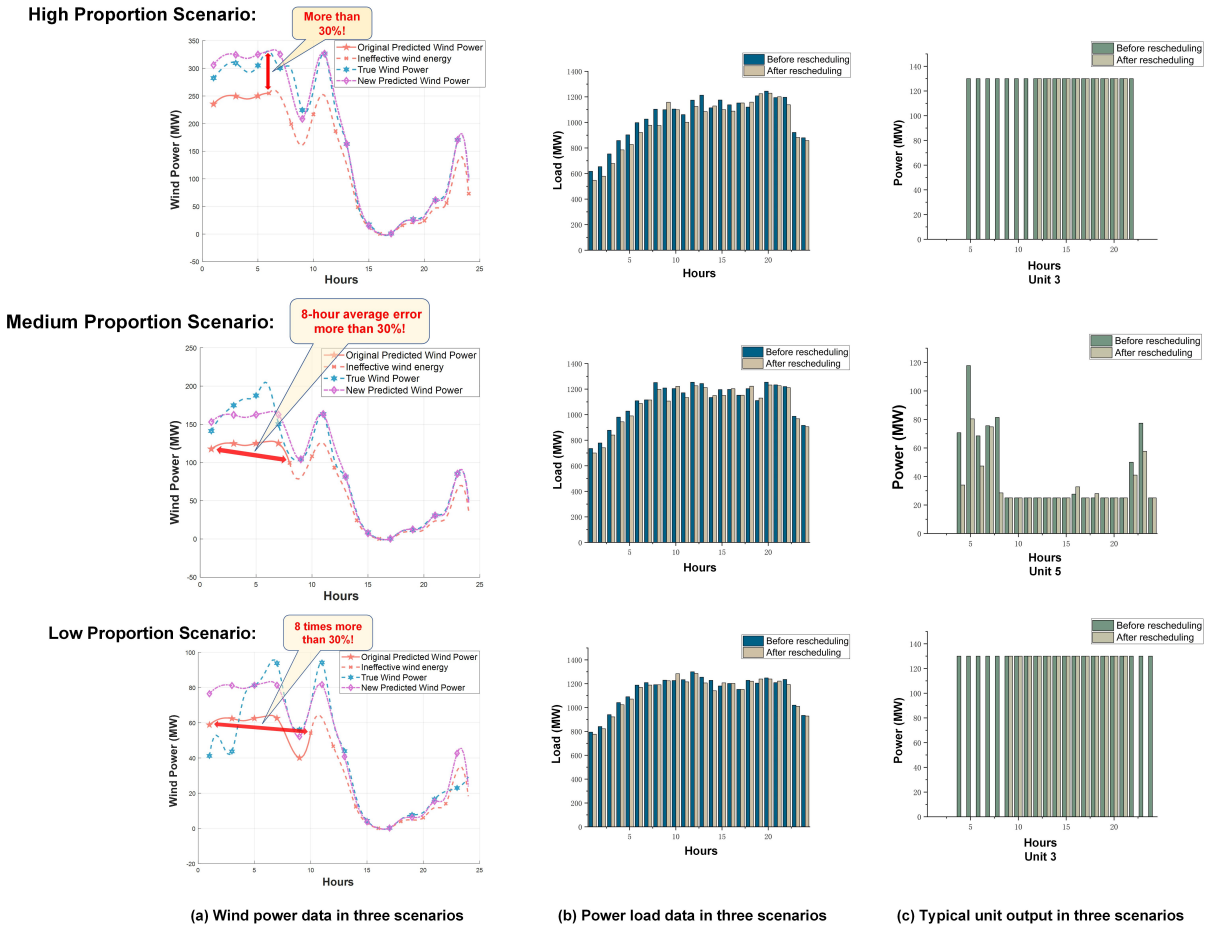

Figure 6: Comparison of three problems in three scenarios.

5. Conclusion

Integrating RGs and PEVs has been a hot topic in the power system operation. In this paper, a power system optimization framework considering wind energy uncertainty has been proposed. This framework uses a group of new MA approaches to realize the intelligent PEV charging and discharging, and addresses

the optimal scheduling of power generating units. In this framework, the predicted wind energy is compared with the actual wind energy in real time, and different application scenarios of wind energy are considered. As long as the difference between the actual wind energy and the predicted wind energy exceeds the threshold, the power system will be actively rescheduled according to the new forecast wind power, so as to reduce the negative effects of the wind power uncertainty on the electric power system.

In order to verify the effectiveness of the proposed method, three case studies have been conducted. The experimental results confirm the effectiveness of the proposed method in solving the power system scheduling problems with uncertain renewable energy sources, achieving up to over 5.3% cost reduction. The mass roll-out of PEVs and significant penetration of wind energy will play an increasingly important role in the future energy system and the decarbonization journey worldwide. Actively rescheduling the power system can significantly improve the economic performance and provide a buffer scheme for the relief of the uncertainty of RGs. The potentials of PEVs can also be leveraged through proper scheduling. In addition, the future work will consider the use of wind energy prediction algorithms to further increase the accuracy of predicting wind energy, and further refine the indicators and thresholds of wind energy in order to be closer to actual application scenarios.

Acknowledgments

National Science Foundation of China under grants 52077213 and 62003332, and Outstanding Young Researcher Innovation Fund of Shenzhen Institute of Advanced Technology, Chinese Academy of Sciences (2018-22).

References

[1] Zhang, L., Li, Y., Zhang, H., Xu, X., Yang, Z., Xu, W.: A review of the potential of district heating system in northern china. Applied Thermal Engineering **188** (2021) 116605
[2] Figueres, C., Le Quéré, C., Mahindra, A., Bäte, O., Whiteman, G., Peters, G., Guan, D.: Emissions are still rising: ramp up the cuts. Nature **564**(7734) (2018) 27–30
[3] Saber, A.Y., Venayagamoorthy, G.K.: Plug-in vehicles and renewable energy sources for cost and emission reductions. IEEE Transactions on Industrial Electronics **58**(4) (2011) 1229–1238
[4] Li, Y., Wang, P., Gooi, H.B., Ye, J., Wu, L.: Multi-objective optimal dispatch of microgrid under uncertainties via interval optimization. IEEE Transactions on Smart Grid **10**(2) (2019) 2046–2058
[5] Zheng, Q.P., Wang, J., Liu, A.L.: Stochastic optimization for unit commitment—a review. IEEE Transactions on Power Systems **30**(4) (2015) 1913–1924
[6] Woeginger, G.J.: Exact algorithms for np-hard problems: A survey. In: Combinatorial optimization—eureka, you shrink! Springer (2003) 185–207
[7] Snyder, Walter L., J., Powell, H. David, J., Rayburn, J.C.: Dynamic programming approach to unit commitment. IEEE Transactions on Power Systems **2**(2) (2007) 339–348
[8] Muckstadt, J.A., Wilson, R.C.: An application of mixed-integer programming duality to scheduling thermal generating systems. IEEE Transactions on Power Apparatus and Systems **PAS-87**(12) (1968) 1968–1978
[9] Alemany, J., Magnago, F., Moitre, D., Pinto, H.: Symmetry issues in mixed integer programming based unit commitment. International Journal of Electrical Power and Energy Systems **54**(1) (2014) 86–90
[10] Garver, L.L.: Power generation scheduling by integer programming-development of theory. Transactions of the American Institute of Electrical Engineers Part III Power Apparatus and Systems **81**(3) (1962) 730–734
[11] Cohen, A.I., Yoshimura, M.: A branch-and-bound algorithm for unit commitment. Power Apparatus and Systems IEEE Transactions on **PAS-102**(2) (1983) 444–451
[12] Zhuang, F., Galiana, F.D.: Towards a more rigorous and practical unit commitment by lagrangian relaxation. IEEE Trans Power Syst **3**(2) (1988) 763–773
[13] Jiang, Q., Zhou, B., Zhang, M.: Parallel augment lagrangian relaxation method for transient stability constrained unit commitment. IEEE Transactions on Power Systems **28**(2) (2013) 1140–1148
[14] Yang, Z., Li, K., Niu, Q., Xue, Y.: A comprehensive study of economic unit commitment of power systems integrating various renewable generations and plug-in electric vehicles. Energy Conversion and Management **132** (2017) 460–481
[15] Zhuang, F., Galiana, F.D.: Unit commitment by simulated annealing. IEEE Trans Power Syst **5**(1) (1990) 311–318
[16] Nemati, M., Braun, M., Tenbohlen, S.: Optimization of unit commitment and economic dispatch in microgrids based on genetic algorithm and mixed integer linear programming. Applied Energy **210** (2018) 944–963
[17] Yu, K., Liang, J., Qu, B., Luo, Y., Yue, C.: Dynamic selection preference-assisted constrained multiobjective differential evolution. IEEE Transactions on Systems, Man, and Cybernetics: Systems (2021) 1–12
[18] Yu, K., Liang, J., Qu, B., Yue, C.: Purpose-directed two-phase multiobjective differential evolution for constrained multiobjective optimization. Swarm and Evolutionary Computation **60** (2021) 100799

[19] Simon, S.P., Padhy, N.P., Anand, R.S.: An ant colony system approach for unit commitment problem. International Journal of Electrical Power and Energy Systems **28**(5) (2006) 315–323
[20] Zhao, H., Liu, L.Y., Zhang, G.X.: Optimal design of power system stabilizer using particle swarm optimization. Power System Technology **30**(3) (2006) 32–35
[21] Zhu, X., Zhao, S., Yang, Z., Zhang, N., Xu, X.: A parallel meta-heuristic method for solving large scale unit commitment considering the integration of new energy sectors. Energy (2021) 121829
[22] Hussein, B.M., Jaber, A.S.: Unit commitment based on modified firefly algorithm. Measurement and Control **53**(3-4) (2020) 320–327
[23] de Mars, P., O'Sullivan, A.: Applying reinforcement learning and tree search to the unit commitment problem. Applied Energy **302** (2021) 117519
[24] Yuan, X., Su, A., Nie, H., Yuan, Y., Wang, L.: Application of enhanced discrete differential evolution approach to unit commitment problem. Energy Conversion and Management **50**(9) (2009) 2449–2456
[25] Wang, Y., Yang, Z., Mourshed, M., Guo, Y., Niu, Q., Zhu, X.: Demand side management of plug-in electric vehicles and coordinated unit commitment: A novel parallel competitive swarm optimization method. Energy conversion and management **196** (2019) 935–949
[26] Yuan, X., Ji, B., Zhang, S., Tian, H., Hou, Y.: A new approach for unit commitment problem via binary gravitational search algorithm. Applied Soft Computing **22** (2014) 249–260
[27] Zhai, F., Shi, L.: Solution proposal to the unit commitment problem incorporating manifold uncertainties. IET Generation, Transmission and Distribution **14**(21) (2020) 4763–4774
[28] Rezaee Jordehi, A.: Dynamic environmental-economic load dispatch in grid-connected microgrids with demand response programs considering the uncertainties of demand, renewable generation and market price. International Journal of Numerical Modelling: Electronic Networks, Devices and Fields (2020)
[29] Li, Y., Wang, P., Gooi, H.B., Ye, J., Wu, L.: Multi-objective optimal dispatch of microgrid under uncertainties via interval optimization. IEEE Transactions on Smart Grid **10**(2) (2017) 2046–2058
[30] Holttinen, H., Meibom, P., Orths, A., Lange, B., O'Malley, M., Tande, J.O., Estanqueiro, A., Gomez, E., Söder, L., Strbac, G., et al.: Impacts of large amounts of wind power on design and operation of power systems, results of iea collaboration. Wind Energy **14**(2) (2011) 179–192
[31] Quan, H., Srinivasan, D., Khambadkone, A.M., Khosravi, A.: A computational framework for uncertainty integration in stochastic unit commitment with intermittent renewable energy sources. Applied Energy **152** (2015) 71–82
[32] Lin, Z., Chen, H., Wu, Q., Huang, J., Li, M., Ji, T.: A data-adaptive robust unit commitment model considering high penetration of wind power generation and its enhanced uncertainty set. International Journal of Electrical Power & Energy Systems **129** (2021) 106797
[33] Diuana, F.A., Viviescas, C., Schaeffer, R.: An analysis of the impacts of wind power penetration in the power system of southern brazil. Energy **186** (2019) 115869
[34] Isuru, M., Hotz, M., Gooi, H., Utschick, W.: Network-constrained thermal unit commitment for hybrid ac/dc transmission grids under wind power uncertainty. Applied Energy **258** (2020) 114031
[35] Jin, J., Zhou, P., Zhang, M., Yu, X., Din, H.: Balancing low-carbon power dispatching strategy for wind power integrated system. Energy **149** (2018) 914–924
[36] Hirth, L., Ziegenhagen, I.: Balancing power and variable renewables: Three links. Renewable and Sustainable Energy Reviews **50** (2015) 1035–1051
[37] G. Cobos, N., Arroyo, J.M., Alguacil, N., Street, A.: Network-constrained unit commitment under significant wind penetration: A multistage robust approach with non-fixed recourse. Applied Energy **232** (2018) 489–503
[38] Zhou, Y., Zhai, Q., Yuan, W., Wu, J.: Capacity expansion planning for wind power and energy storage considering hourly robust transmission constrained unit commitment. Applied Energy **302** (2021) 117570
[39] Shang, W.L., Chen, J., Bi, H., Sui, Y., Chen, Y., Yu, H.: Impacts of covid-19 pandemic on user behaviors and environmental benefits of bike sharing: A big-data analysis. Applied Energy **285** (2021) 116429
[40] Zepter, J.M., Weibezahn, J.: Unit commitment under imperfect foresight – the impact of stochastic photovoltaic generation. Applied Energy **243** (2019) 336–349
[41] Bi, H., Shang, W.L., Chen, Y., Wang, K., Yu, Q., Sui, Y.: Gis aided sustainable urban road management with a unifying queueing and neural network model. Applied Energy **291** (2021) 116818
[42] Zhou, B., Zhang, K., Chan, K.W., Li, C., Gao, X.: Optimal coordination of electric vehicles for virtual power plants with dynamic communication spectrum allocation. IEEE Transactions on Industrial Informatics **PP**(99) (2020) 1–1
[43] Hu, Q., Li, H., Bu, S.: The prediction of electric vehicles load profiles considering stochastic charging and discharging behavior and their impact assessment on a real uk distribution network. Energy Procedia **158** (2019) 6458–6465
[44] Pascal, C., Panescu, D.: On rescheduling in holonic manufacturing systems. Computers in Industry **104** (2019) 34–46
[45] Zhang, J., Qin, W., Wu, L., Zhai, W.: Fuzzy neural network-based rescheduling decision mechanism for semiconductor manufacturing. Computers in Industry **65**(8) (2014) 1115–1125
[46] Xu, Y., Han, X., Yang, M., Wang, M., Zhu, X., Zhang, Y.: Condition-based midterm maintenance scheduling with rescheduling strategy. International Journal of Electrical Power & Energy Systems **118** (2020) 105796
[47] Luo, W., Jin, M., Su, B., Lin, G.: An approximation scheme for rejection-allowed single-machine rescheduling. Computers & Industrial Engineering **146** (2020) 106574
[48] Altazin, E., Dauzère-Pérès, S., Ramond, F., Tréfond, S.: A multi-objective optimization-simulation approach for real time rescheduling in dense railway systems. European Journal of Operational Research **286**(2) (2020) 662–672
[49] Li, C.L., Li, F.: Rescheduling production and outbound deliveries when transportation service is disrupted. European Journal of Operational Research **286**(1) (2020) 138–148

[50] Kuppusamy, P., Venkatraman, S., Rishikeshan, C., Padmanabha Reddy, Y.: Deep learning based energy efficient optimal timetable rescheduling model for intelligent metro transportation systems. Physical Communication **42** (2020) 101131
[51] Nasiri, M.M., Ahmadi, N., Konur, D., Rahbari, A.: A predictive-reactive cross-dock rescheduling system under truck arrival uncertainty. Expert Systems with Applications **188** (2022) 115986
[52] Zhan, S., Wang, P., Wong, S., Lo, S.: Energy-efficient high-speed train rescheduling during a major disruption. Transportation Research Part E: Logistics and Transportation Review **157** (2022) 102492
[53] Wang, T., Tang, Y.: Transfer-reinforcement-learning-based rescheduling of differential power grids considering security constraints. Applied Energy **306** (2022) 118121
[54] Lund, H., Kempton, W.: Integration of renewable energy into the transport and electricity sectors through v2g. Energy policy **36**(9) (2008) 3578–3587
[55] Gaing, Z.L.: Discrete particle swarm optimization algorithm for unit commitment. In: Power Engineering Society General Meeting. (2003) 424 Vol. 1
[56] Kazarlis, S.A., Bakirtzis, A.G., Petridis, V.: A genetic algorithm solution to the unit commitment problem. Power Systems IEEE Transactions on **11**(1) (1996) 83–92
[57] Yang, Z., Li, K., Guo, Y., Feng, S., Niu, Q., Xue, Y., Foley, A.: A binary symmetric based hybrid meta-heuristic method for solving mixed integer unit commitment problem integrating with significant plug-in electric vehicles. Energy **170** (2019) 889–905
[58] Cheng, R., Jin, Y.: A social learning particle swarm optimization algorithm for scalable optimization. Information Sciences **291**(C) (2015) 43–60
[59] Yang, Z., Li, K., Niu, Q., Xue, Y.: A novel parallel-series hybrid meta-heuristic method for solving a hybrid unit commitment problem. Knowledge-Based Systems **134** (2017) 13–30